



ELSEVIER

# Synergistic encapsulation of the anti-HIV agent efavirenz within mixed poloxamine/poloxamer polymeric micelles

Diego A. Chiappetta, PhD<sup>a,b</sup>, Graciela Facorro, PhD<sup>c</sup>,  
Emilio Rubin de Celis, BSc<sup>c</sup>, Alejandro Sosnik, PhD<sup>a,b,\*</sup>

<sup>a</sup>The Group of Biomaterials and Nanotechnology for Improved Medicines (BIONIMED), Department of Pharmaceutical Technology, Faculty of Pharmacy and Biochemistry, University of Buenos Aires, Argentina

<sup>b</sup>National Science Research Council (CONICET)

<sup>c</sup>Department of Physics, Faculty of Pharmacy and Biochemistry, University of Buenos Aires, Argentina

Received 28 July 2010; accepted 30 January 2011

## Abstract

This study investigated the synergistic performance of mixed polymeric micelles made of linear and branched poly(ethylene oxide)-poly(propylene oxide) for the more effective encapsulation of the anti-HIV drug efavirenz. The co-micellization process of 10% binary systems combining different weight ratios of a highly hydrophilic poloxamer (Pluronic F127) and a more hydrophobic poloxamine counterpart (Tetronic T304 and T904) was investigated by means of dynamic light scattering, cloud point and electronic spin resonance experiments. Then, the synergistic solubilization capacity of the micelles was shown. Findings revealed a sharp solubility increase from 4 µg/ml up to more than 33 mg/ml, representing a 8430-fold increase. Moreover, the drug-loaded mixed micelles displayed increased physical stability over time in comparison with pure poloxamine ones. Overall findings confirmed the enormous versatility of the poloxamer/poloxamine systems as Trojan nanocarriers for drug encapsulation and release by the oral route and they entail a relevant enhancement of the previous art towards a more compliant pediatric HIV pharmacotherapy.

**From the Clinical Editor:** In this study, the authors demonstrate the versatility of poloxamer/poloxamine systems as Trojan nanocarriers for anti-HIV drug encapsulation and release by the oral route. A highly relevant stability and solubility enhancement is shown, which may ultimately lead to more compliant anti-HIV pharmacotherapy.

© 2011 Elsevier Inc. All rights reserved.

**Key words:** Poloxamer/poloxamine mixed polymeric micelles; Micellar fluidity and polarity; Electronic spin resonance (ESR); Pediatric HIV/AIDS pharmacotherapy; Synergistic efavirenz encapsulation

The Human Immunodeficiency Virus (HIV)/Acquired Immunodeficiency Syndrome (AIDS) is the most deadly infectious disease of our times with approximately 40 million infected patients worldwide.<sup>1</sup> The number of infected children is approximately 2.5 million, 60% of them living in the sub-Saharan region (SSR) of Africa.<sup>1</sup>

The High Activity Antiretroviral Therapy (HAART) is composed of the chronic administration of high and frequent doses of at least 3 antiretrovirals (ARV).<sup>2,3</sup> A successful pharmacotherapy demands adherence levels greater than 95%.<sup>4</sup>

Pediatric HIV is rare in developed countries.<sup>5</sup> In contrast, a new thousand cases are recorded daily in developing nations.

Only 10% of the infected children have appropriate access to the ARV medications (fewer than 2% in the SSR).<sup>6</sup> About 15 million children have been orphaned due to AIDS in Africa (11.6 millions in the SSR).<sup>7</sup> In this context, a majority of the pediatric patients will probably succumb to the disease within the first two years of life.

One of the main hurdles faced in pediatric HIV is the small number of approved drugs.<sup>8</sup> In addition, the limited availability of commercial liquid formulations makes dose adjustment and oral administration more challenging than for other forms of medications.<sup>9</sup> The World Health Assembly proclaimed the right of children to access to safe, effective and proven medicines.<sup>10</sup> However, the large-scale development of more appropriate pediatric medications constitutes a pending agenda in HIV/AIDS, and only marginal progress has been in evidence since that proclamation.<sup>11</sup>

Efavirenz (EFV) is a poorly water-soluble (intrinsic solubility = 4 µg/mL) first-line non-nucleoside reverse transcriptase

The work was supported by the University of Buenos Aires (Grant UBACyT 20020090200016) and CONICET (Grant PIP 11220090100220).

No conflict of interest is present.

\*Corresponding author.

E-mail address: alesosnik@gmail.com (A. Sosnik).

inhibitor employed in the pharmacotherapy of children above 3 years of age.<sup>12–14</sup> It displays intermediate oral bioavailability (40–45%) and relatively high intra- (55–58%) and inter-individual variability (19–24%).<sup>15,16</sup>

Therapeutic Drug Monitoring (TDM) of EFV is recommended to adjust the dose to body weight and to prevent adverse effects and treatment cessation.<sup>17,18</sup>

The only commercial EFV formulation is a concentrated (30 mg/mL) medium-chain triglyceride (MCT, Miglyol 82) solution.<sup>19</sup> The oral bioavailability of the drug is approximately 20% less than that of capsules. In addition, chronic MCT oral administration produced reversible diarrhea and weight loss in rats.<sup>20</sup> Thus, this pharmaceutical excipient does not seem to be the most appropriate one for children in chronic treatment. This formulation is not registered by the national regulatory agency of Argentina<sup>21</sup> and most of the children are still administered solid medicines.

The development of innovative, scalable and cost-effective anti-HIV medicines is a crucial stage to improve the course of the disease, especially in children.<sup>14,22,23</sup>

Polymeric micelles are appealing Trojan horses to make water soluble hydrophobic drugs intended for oral administration.<sup>24</sup> The thermo-responsive poly(ethylene oxide)–poly(propylene oxide) (PEO–PPO) block copolymers are the most popular micelle-forming amphiphiles.<sup>25–27</sup> We recently reported on the efficient encapsulation of EFV in pure micelles of pristine and modified PEO-PPO copolymers<sup>28,29</sup> and developed a stable taste-masked formulation. The oral bioavailability of the drug was improved significantly.<sup>28</sup> A greater drug concentration would represent an additional noteworthy feature to reduce the administered volume and to enhance patient compliance and adherence. However, T904 pure micelles containing high EFV payloads are not physically stable over time.<sup>28–30</sup>

Mixed polymeric micelles are generated by the co-micellization of two amphiphiles displaying different hydrophilic-lipophilic balance (HLB) and have become an effective approach to optimize the encapsulation performance of poorly water-soluble drugs and the physical stability of the systems.<sup>31,32</sup> Aiming to further explore and expand the versatility of PEO-PPO systems as valuable nanotechnology tools in the development of innovative, scalable and cost-effective medicines in HIV and other neglected diseases, this study primarily investigated the self-aggregation behavior of poloxamer/poloxamine mixed micelles by means of dynamic light scattering (DLS) and electron spin resonance (ESR). Then, the synergistic encapsulation of EFV within F127:T904 binary systems was confirmed. The drug-loaded mixed micelles displayed noticeably greater physical stability than did the pure counterpart. The developed systems entail a further enhancement of the previous art toward a more compliant pediatric HIV pharmacotherapy.

## Methods

### Materials

Poloxamer Pluronic® F127 (MW 12.6 kDa, 70 wt% PEO, HLB 18–23) and poloxamines Tetronic® 304 (T304, MW 1.65

kDa, 40 wt% PEO, HLB 12–18) and 904 (T904, MW 6.7 kDa, 40 wt% PEO, HLB 12–18) were a gift of BASF (Mount Olive, New Jersey). Efavirenz (LKM Laboratories, Buenos Aires, Argentina) and other reagents and solvents were of analytical grade and were used as received.

### Preparation of mixed polymeric micelles

To prepare mixed F127:T304 and F127:T904 polymeric micelles (10% weight/volume total concentration, 75:25, 50:50 and 25:75 copolymer weight ratios), the required amount of each copolymer was first dissolved in phosphate-citrate buffer solution (pH 5.0) at 4°C and then the system was equilibrated at 25°C. Pure F127, T304 and T904 (10%) controls are denoted pF127, pT304 and pT904, respectively.

### DLS

The average hydrodynamic diameter ( $D_h$ ) and the size distribution were measured by DLS (Zetasizer Nano-Zs, Malvern Instruments, Worcestershire, United Kingdom) provided with a He-Ne (633 nm) laser and a digital correlator ZEN3600, at 25° and 37°C. Measurements were conducted at a scattering angle of  $\theta = 173^\circ$  to the incident beam. Results are expressed as the average of 5 measurements. DLS was employed to establish the critical micellar concentration (CMC), at 25° and 37°C. Twenty copolymer solutions covering a concentration range between 0.001–5% were prepared in phosphate-citrate buffer solution (pH 5.0). The CMC value corresponds to the concentration of the pure or the binary system at which a sharp increase in the scattering intensity occurred.<sup>33</sup>

### Cloud point (CP)

CP measurements were conducted by submerging sealed glass vials that contained each micellar system (10%) in an oil bath at room temperature. Then, the temperature was increased gradually from 22°C (1°C/minute) until the point of abrupt change in the visual appearance of the system from clear to turbid.<sup>34</sup> Assays were carried out in duplicate. The maximum uncertainty in the CP measurement was  $\pm 1^\circ\text{C}$ .

### ESR

The fluidity and the polarity of drug-free micelles were investigated by means of ESR using stearic acid markers that bear the nitroxide radical on two different positions, namely 5-doxyl stearic acid (5DSA) and 16-doxyl stearic acid (16DSA). Pure and mixed micelles (10%, 400  $\mu\text{L}$ ) were mixed with aqueous solutions of 5DSA (1.0 mM, 20  $\mu\text{L}$ ) or 16DSA (4.4 mM, 20  $\mu\text{L}$ ) and divided into 2 fractions (180  $\mu\text{L}$  each). Then, fractions 1 and 2 were diluted with distilled water (60  $\mu\text{L}$ ) and  $\text{K}_3\text{Fe}(\text{CN})_6$  (0.8 mM in water, 60  $\mu\text{L}$ ), respectively; the polar paramagnetic  $\text{K}_3\text{Fe}(\text{CN})_6$  was used as the broadening agent of the spin label. Preliminary assays were performed with the water-soluble 2,2,6,6-tetramethylpiperidine 1-oxyl (TEMPO). The nitroxide radical ESR signal was detected using an X-band ESR spectrometer Bruker ECS 106 (Bruker, Rheinstetten, Germany) at 25°C using an ESR aqueous flat cell. The spectrometer settings for the nitroxide radicals were: field center 3450 Gauss, sweep width 100 Gauss, microwave power 10 mW,

time constant 5.12 ms, conversion time 5.12 ms, modulation frequency 50 kHz, modulation amplitude 0.7 Gauss, and resolution 1024 points. The nitroxide radical signal intensity was measured considering the value of the double integral of the  $^{14}\text{N}$  triplet. All spectra are the accumulation of 15 scans.

#### Morphology of mixed polymeric micelles

The morphology of drug-free F127:T904 (50:50) mixed micelles was characterized by means of transmission electron microscopy (TEM, Philips CM-12 TEM apparatus, FEI Company, Eindhoven, The Netherlands) by negatively staining with 2% phosphotungstic acid solution.<sup>28</sup>

#### Encapsulation of EFV

EFV (in excess) was added to micellar suspensions (3 mL) and samples were shaken (48 hours) at 25°C. The resulting suspensions were filtered (0.45  $\mu\text{m}$ , cellulose nitrate) to remove insoluble EFV. The EFV concentration was determined by UV spectrophotometry (247 nm, CARY [IE] UV–Visible Spectrophotometer, Varian, Palo Alto, California) using a calibration curve of EFV methanolic solutions (4–20  $\mu\text{g/mL}$ ). The correlation factor was 0.9998–1.0000. A drug-free copolymer methanolic solution was used as blank. Solubility factors ( $f_s$ ) were calculated according to the equation

$$f_s = S_a / S_{\text{water}}$$

$S_a$  and  $S_{\text{water}}$  being the EFV apparent solubility in micelles and the intrinsic solubility in buffer (4  $\mu\text{g/mL}$ ). The size and size distribution of the drug-loaded micelles was determined by DLS at 25° and 37°C (see above).

An aliquot of EFV-loaded F127 micelles (10%) was freeze-dried and was redissolved in deuterium dioxide ( $\text{D}_2\text{O}$ ) or deuterated dimethyl sulfoxide ( $\text{DMSO-d}_6$ ), and analyzed by proton nuclear magnetic resonance ( $^1\text{H-NMR}$ , Varian 200MHz spectrometer) at room temperature.

#### Physicochemical stability of drug-containing micelles

EFV-loaded specimens were stored at 25°C and monitored over 28 days. To determine the EFV remaining in solution, samples were processed as described above. The percentage of remaining EFV (% EFV) was calculated and expressed as mean  $\pm$  standard deviation (SD) ( $n = 3$ ). In tandem, the size and size distribution of the drug-loaded aggregates were assessed by DLS (see above).

#### Data analysis

Values are represented as the mean  $\pm$  SD. The statistical analysis was performed by a one-way ANOVA (5% significance level, P values smaller than 0.05 were considered statistically insignificant) combined with the Dunnett Multiple Comparison Test or t-test (5% significance level, P values smaller than 0.05 were considered statistically insignificant). The software was GraphPad Prism version 5.00 for Windows (GraphPad Software).

Table 1  
Structural characteristics of the linear and branched PEO-PPO amphiphiles chosen for the study

Copolymer	Molecular weight (kDa)*	$N_{\text{EO}}^{\dagger}$	$N_{\text{PO}}^{\ddagger}$	PPO (wt %)	EO/PO molar ratio	Chemical structure
F127	12.60	200.5	65.2	30	3.08	$\text{HOCH}_2\text{-CH}_2\text{-(O-CH}_2\text{-CH}_2\text{)}_{a-1}\text{-(CH-CH}_2\text{-O)}_b\text{-(CH}_2\text{-CH}_2\text{-O)}_{a-1}\text{-CH}_2\text{-CHOH}$ 
T304	1.65	15.0	17.1	60	0.88	$\text{HOCH}_2\text{-CH}_2\text{-(O-CH}_2\text{-CH}_2\text{)}_{a-1}\text{-(O-CH}_2\text{-CH)}_b$ 
T904	6.70	60.9	69.3	60	0.88	$\text{HOCH}_2\text{-CH}_2\text{-(O-CH}_2\text{-CH}_2\text{)}_{a-1}\text{-(O-CH}_2\text{-CH)}_b$ 

$N_{\text{EO}}$ , mean number of EO units per PEO block;  $N_{\text{PO}}$ , mean number of PO units per PPO block; EO/PO, molar ratio of EO and PO units calculated as  $N_{\text{EO}}/N_{\text{PO}}$ .

\*Molecular weight of the copolymers as reported by BASF.  $^{\dagger}$ Chiappetta and Sosnik.<sup>25</sup>

F127 is a highly hydrophilic poloxamer, and poloxamines T304 and T904 are derivatives of similar intermediate hydrophilicity and different PPO block molecular weights.

Table 2  
CMC and CP values for micellar systems in buffer phosphate-citrate

Copolymers	Composition % (A:B)*	CMC				CP (°C)
		25°C		37°C		
		Theoretical value <sup>†</sup> (mM)	Experimental value <sup>‡</sup> (mM)	Theoretical value <sup>†</sup> (mM)	Experimental value <sup>‡</sup> (mM)	
pF127	100:0	-	0.240	-	0.010	109
F127:T304	75:25	0.817	0.886	0.035	0.027	108
	50:50	1.840	2.742	0.085	0.069	106
	25:75	4.161	5.693	0.230	0.237	94
pT304	0:100	-	14.500	-	6.100	88
F127:T904	75:25	0.293	0.281	0.015	0.019	104
	50:50	0.345	0.400	0.023	0.025	97
	25:75	0.398	0.527	0.038	0.038	80
pT904	0:100	-	0.450	-	0.075	75

A good agreement between the theoretical and experimental CMC was observed, at 25° and 37°C. Moreover, single CP values indicated the generation of mixed micelles.

\* Percentage of hydrophilic poloxamer F127 (A):percentage of hydrophobic poloxamine (B) (A:B: e.g., F127:T304).

<sup>†</sup> Theoretical value calculated by Equation 1.

<sup>‡</sup> Experimental value determined by DLS.

## Results

### Self-aggregation of mixed polymeric micelles

Aiming to explore the generation of poloxamer/poloxamine mixed polymeric micelles, 3 amphiphiles were employed. F127 is a highly hydrophilic poloxamer, and poloxamines T304 and T904 are derivatives of similar intermediate hydrophilicity and different PPO block molecular weights (Table 1). In addition, F127 and T904 present different EO/PO molar ratios, though PPO segments of approximately 4 kDa (Table 1). F127 and T304 display disimilar hydrophobicity and PPO blocks.

The CMC of pure and mixed systems was determined by DLS. The theoretical CMC value for a mixed surfactant system, CMC\*, can be calculated using the following equation.<sup>35</sup>

$$1/\text{CMC}^* = X_1/\text{CMC}_1 + X_2/\text{CMC}_2 \quad (1)$$

$X_1$  and  $X_2$  being the molar fractions of the components 1 and 2, and  $\text{CMC}_1$  and  $\text{CMC}_2$  the CMC values of components 1 and 2, respectively. The good agreement between the theoretical and experimental data at 25° and 37°C is shown in Table 2. In general, the incorporation of poloxamine to pF127 micelles resulted in the gradual increase of the theoretical and the experimental CMC of the mixtures (Figure 1). At 25°C, the experimental CMC was consistently greater than the theoretical one. Differences are more notorious for F127:T304 systems. T904-containing systems showed a similar behavior. Conversely, the CMC of the mixed systems was smaller than that of pT304 and pT904. At 37°C, CMC values of the mixed systems were also greater than that of pF127. However, a stronger aggregation tendency was apparent. Only 25% F127 content in F127:T304 (25:75) decreased the CMC of pT304 from 6.100 to 0.237 mM. For F127:T304 systems, the experimental CMC values were smaller than the theoretical ones, showing a negative deviation from ideal behavior. Conversely, T904-containing systems showed a positive deviation (Figure 1).

### CP

Table 2 summarizes the data of different pure and mixed micelles. Single CP values were observed. pF127 showed a CP of 109°C, in good agreement with the literature.<sup>36</sup> pT304 and pT904 showed a lower CP, values being 88° and 75°C, respectively; for similar EO/PO, the higher the molecular weight, the lower the CP. Then, the steady increase of the poloxamine content in the binary system resulted in the concomitant decrease of the CP, indicating a stronger aggregation tendency (Table 2). On the other hand, all the binary systems showed higher CP than the corresponding pure poloxamine owing to the hydrophilic contribution of F127.

### Micellar size and size distribution

At 25°C, pF127 displayed a bimodal intensity fraction distribution (Table 3). The smaller fraction (peak 1,  $D_h = 6.1$  nm, 23%) would correspond to unimers or incomplete aggregates and the major one (peak 2,  $D_h = 39.3$  nm, 77%) to polymeric micelles.<sup>27</sup> A PDI value of 0.47 was consistent with a bimodal distribution (Figure S1). F127:T304 mixtures generated mainly large aggregates of  $D_h$  between 35.0–41.7 nm (> 90%), sizes gradually growing for increasing T304 concentrations. The tiny fraction of small  $D_h$  fitted the size of T304 unimers (2.7 nm); T304 requires a remarkably greater concentration to aggregate because of an especially low molecular weight.<sup>27</sup> In addition, PDI values decreased from 0.31 to 0.26 for 75:25 and 25:75 systems. These findings would suggest that T304 enhances the F127 self-aggregation. At 25°C, pT904 combined a major small-size fraction (peak 1,  $D_h = 5.6$  nm, 86.9%) with a minor larger-sized one (peak 2,  $D_h = 303$  nm, 13.1%). The former probably corresponds to small micelles, and the latter was previously ascribed to insoluble residues of the copolymer synthesis.<sup>27</sup> F127:T904 micelles showed a similar trend though sizes were slightly larger than those of pF127 and F127:T304. On the other hand, PDI values of F127:T904 mixed micelles increased



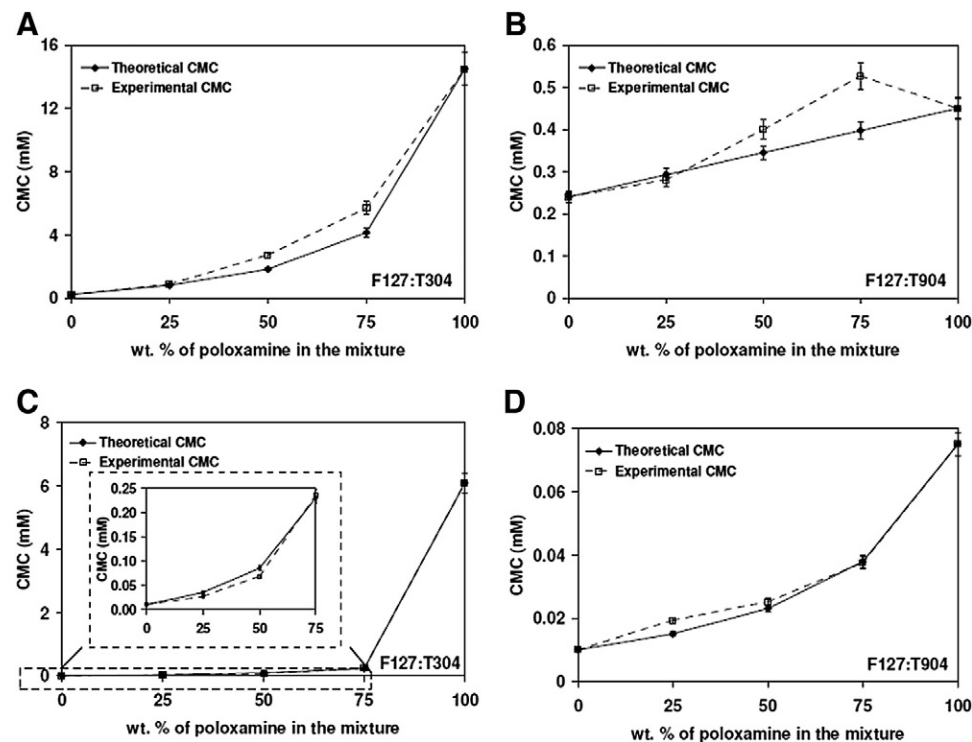


Figure 1. CMC versus percentage of poloxamine in the mixture. (A) F127:T304 and (B) F127:T904, at 25°C. (C) F127:T304 and (D) F127:T904, at 37°C. Positive and negative deviations from ideality suggest unfavorable and favorable mixing processes, respectively.

Table 3

$D_h$  and size distribution of 10% EFV-free micellar systems in buffer phosphate-citrate, at 25° and 37°C

Copolymers	T (°C)	Peak 1		Peak 2		PDI (± S.D.)
		$D_h$ (nm)	%	$D_h$ (nm)	%	
pF127	25	6.1 (0.3)	23.0	39.3 (0.9)	77.0	0.47 (0.00)
F127:T304 (75:25)		4.1 (0.2)	9.6	35.0 (0.5)	90.4	0.31 (0.00)
F127:T304 (50:50)		2.9 (0.2)	5.7	37.4 (0.3)	94.3	0.27 (0.00)
F127:T304 (25:75)		2.6 (0.1)	5.5	41.7 (0.5)	94.5	0.26 (0.01)
pT304		2.7 (0.1)	100.0	-	-	0.16 (0.01)
F127:T904 (75:25)	25	5.6 (0.5)	19.5	38.8 (1.7)	80.5	0.48 (0.01)
F127:T904 (50:50)		5.2 (0.1)	17.5	44.1 (0.6)	82.5	0.55 (0.00)
F127:T904 (25:75)		5.1 (0.1)	19.3	50.3 (0.3)	80.7	0.61 (0.04)
pT904		5.6 (0.1)	86.9	303.6 (42.5)	13.1	0.26 (0.01)
pF127		37	20.4 (0.4)	100.0	-	-
F127:T304 (75:25)	25.4 (0.5)		100.0	-	-	0.23 (0.01)
F127:T304 (50:50)	29.8 (0.5)		100.0	-	-	0.19 (0.01)
F127:T304 (25:75)	37.4 (0.2)		100.0	-	-	0.18 (0.01)
pT304	2.5 (0.1)		27.9	26.9 (1.1)	72.1	0.41 (0.02)
F127:T904 (75:25)	19.3 (0.2)		100.0	-	-	0.25 (0.01)
F127:T904 (50:50)	16.3 (0.2)		100.0	-	-	0.23 (0.01)
F127:T904 (25:75)	14.0 (0.4)		100.0	-	-	0.18 (0.01)
pT904	11.8 (0.2)		100.0	-	-	0.12 (0.01)

At 37°C, all the pure and mixed systems (with the exception of pT304) displayed monomodal size distributions with small PDI values between 0.18–0.25 that are consistent with a complete micellization.

As expected, micelles shrank with respect to the same systems at 25°C.

slightly from 0.48 for 75:25 to 0.61 for 25:75, suggesting some deleterious effect on micellization.

At 37°C, all the pure and mixed systems (with the exception of pT304) displayed monomodal size distributions with small

PDI values between 0.18–0.25 that are consistent with a complete micellization. This was supported by the absence of small-size unimers and partially formed aggregates. In addition, at this higher temperature, pT304 began to micellize; note the

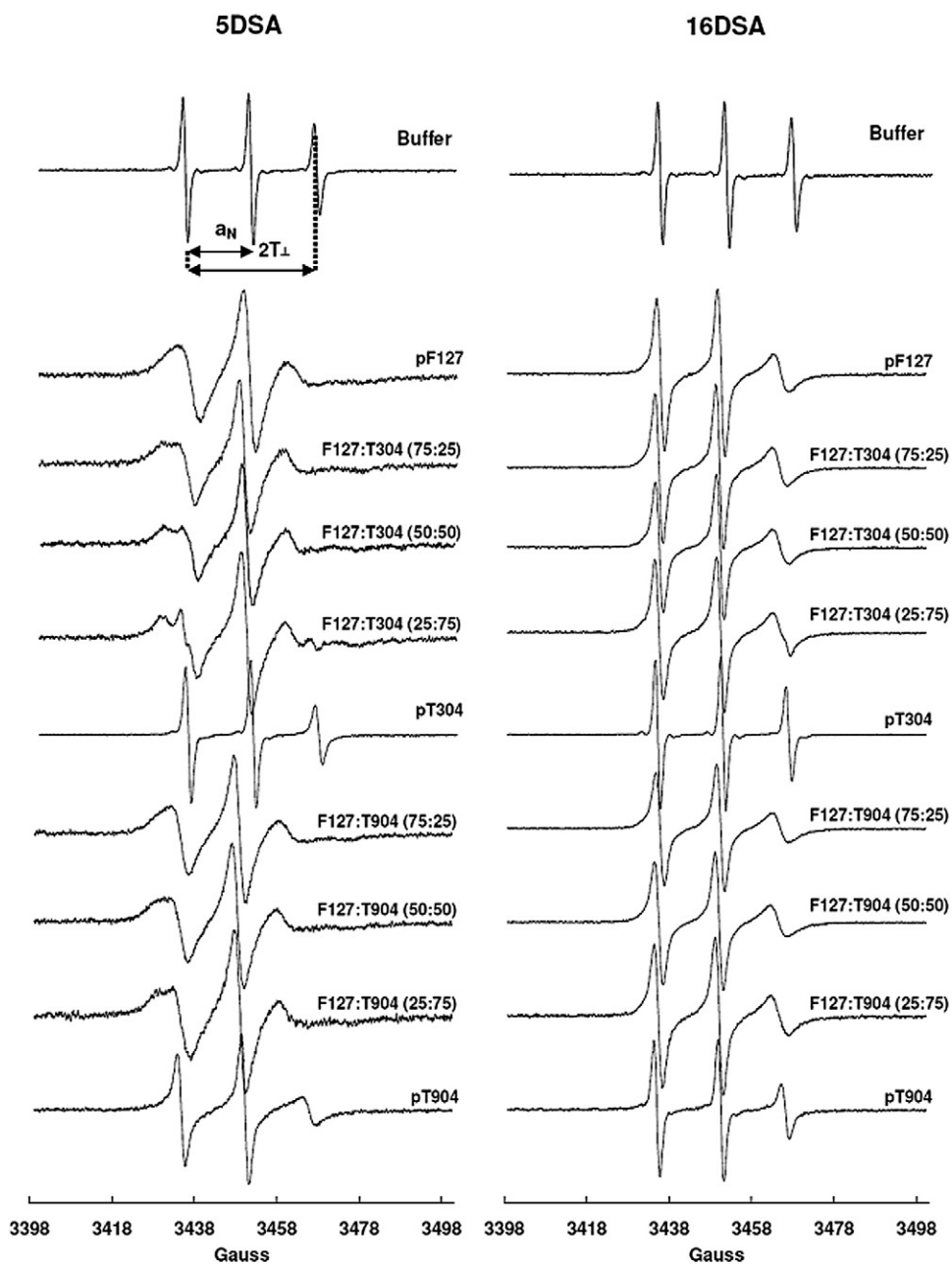


Figure 2. ESR spectra of 5DSA and 16DSA labels in the different micellar systems. The broadening of the peaks due to the incorporation of the label into the micelles is clearly appreciated.

presence of nano-sized structures of 26.9 nm. As expected, micelles shrank with respect to the same systems at 25°C (Table 3), as expressed by the smaller  $D_h$  and PDI values. This phenomenon was especially noticeable for F127:T904 mixtures and it is in full agreement with the greater aggregation tendency of these thermo-responsive biomaterials upon heating.<sup>25</sup> The more constrained temperature-driven shrinkage shown by F127:T304 would rely on the more limited temperature-sensitive nature of this low molecular weight poloxamine.<sup>27</sup> This is supported by the gradual size growth displayed by systems with increasing T304 contents.

#### ESR

ESR is a powerful technique to investigate changes in both the fluidity and the polarity of the microenvironment that might stem from the co-micellization process.<sup>37,38</sup> The former is observed as the broadening of the three characteristic resonance peaks of the label signal due to a more limited molecular mobility and leads to a change in the parameter  $2T_{\perp}$ . The latter alters the hyperfine coupling constant,  $a_N$ .<sup>37</sup> Preliminary assays employed the water-soluble TEMPO, though the spectrum of this label in the different micellar systems was fully conserved,

Table 4  
ESR parameters of 5DSA and 16DSA encapsulated within pure and mixed micelles

Copolymers	% Broadening* ( $\pm$ SD)		2T <sub>L</sub> (Gauss)		a <sub>N</sub> (Gauss)	
	5 DSA	16 DSA	5 DSA	16 DSA	5 DSA	16 DSA
pF127	30	0	20.0	25.7	13.29	14.37
F127:T304 (75:25)	24	0	21.6	25.9	13.39	14.47
F127:T304 (50:50)	22	0	21.1	26.0	13.00	14.47
F127:T304 (25:75)	13	0	21.5	26.3	13.39	14.57
pT304	100	100	29.6	29.9	15.54	15.64
F127:T904 (75:25)	10	0	21.8	25.9	13.78	14.37
F127:T904 (50:50)	12	0	21.4	25.5	13.39	14.37
F127:T904 (25:75)	10	0	20.6	26.1	13.00	14.57
pT904	0	0	28.2	29.0	15.35	15.25

2T<sub>L</sub> is the separation between the inner hyperfine lines. The 2T<sub>L</sub> of 5DSA and 16DSA in water were 30.3 and 30.5, respectively.

a<sub>N</sub>, the hyperfine splitting constant, of 5DSA and 16DSA in water was 15.74. The fluidity and the polarity of the micelles was estimated by measuring 2T<sub>L</sub> and a<sub>N</sub>.

\* Broadening agent: K<sub>3</sub>Fe (CN)<sub>3</sub>.

indicating that it was not incorporated into the micelles. Then, ESR studies involved amphiphilic labels that bear the radical moiety in the proximity of the hydrophilic head (5DSA) or onto the edge of the hydrophobic tail (16DSA). Once 5DSA is incorporated into the polymeric micelle, the nitroxide radical is accommodated within the micellar corona and close to the outer aqueous medium. Conversely, the radical group of 16DSA is expected to be hosted by the micellar core. It is important to note that the interaction between the micelle and the label molecule is not supposed to change due to the presence of the free radical moiety in two different positions along the same stearic acid chain. The broadening of the peaks due to the incorporation of the label into the micelles is clearly appreciated (Figure 2). The 2T<sub>L</sub> and a<sub>N</sub> parameters were calculated for each micelle/label pair and in comparison with the values of the label in a copolymer-free system (Table 4). 5DSA-labelled pF127 and pT904 showed substantially different 2T<sub>L</sub> values of 20.0 and 28.2 Gauss, respectively. These values were smaller than that of the label in buffer (30.3 Gauss). In contrast, the 2T<sub>L</sub> in pT304 was similar to that in buffer, indicating that the label is not incorporated into micelles; T304 does not micellize at 25°C. F127:T304 and F127:T904 mixtures showed 2T<sub>L</sub> similar to pF127, independently of the poloxamine content (Table 4). In addition, a<sub>N</sub> of 5DSA in the binary systems was very similar to that of pF127 and smaller than the values observed in buffer, pT304 and pT904 (Table 4).

With 16DSA, 2T<sub>L</sub>pF127 was lower than that in buffer, pT304 and pT904. The fact that 2T<sub>L</sub>pF127 was smaller than 2T<sub>L</sub>pT904 indicated that the mobility within pF127 micelles is slightly more constrained. Because pT304 does not encapsulate the label, the 2T<sub>L</sub>pT304 was similar to the value in a copolymer-free system. A comparison between 2T<sub>L</sub> data for 5DSA and 16DSA shows that

the former are consistently smaller than the latter, independently of the micellar system. Furthermore, a<sub>N</sub> results of 16DSA encapsulated within mixed micelles were also similar to those in pF127 and smaller than in buffer, pT304 and pT904.

The addition of a paramagnetic broadening agent did not quench the signal of 16DSA (% broadening = 0%) in any of the specimens, indicating that regardless of the micellar composition, the label is completely incorporated into the micelles and “protected” from the quencher (Table 4). pT304 did not self-assemble under the conditions of the experiment (25°C); thus, both labels remained exclusively in the aqueous medium and the signal was totally quenched by K<sub>3</sub>Fe(CN)<sub>3</sub> (Table 4). In the case of 5DSA, pT904 micelles totally prevented the broadening phenomenon. Conversely, pF127 micelles prevented the broadening phenomenon only partially (% broadening = 30%). The gradual increase of T304 concentration in the F127:T304 mixed micelles reduced the quenching extent from 30% (for 0% poloxamine) to 13% (for 75% poloxamine). A smaller broadening extent suggested that more hydrophobic micelles prevent more efficiently the diffusion of the quencher from the aqueous medium into the micelle. A similar behavior was observed with F127:T904 systems, though the quenching percentage decreased sharply to 10% upon the aggregation of only 25 wt % poloxamine. The percent broadening for systems containing greater T904 contents remained constant between 10–12%.

#### Morphology of mixed polymeric micelles

The spherical morphology of the mixed micelles was confirmed by TEM analysis, as exemplified for F127:T904 (50:50) in Figure S2.

#### Solubilization of EFV into PEO-PPO mixed polymeric micelles

Encapsulation assays were carried out with systems containing total copolymer concentrations far above the CMC previously established (Table 2). This ensured the presence of micelles. To confirm that EFV is primarily hosted by the micellar core, EFV-loaded pF127 micelles were analyzed by <sup>1</sup>H NMR (Figure S3). In DMSO-*d*<sub>6</sub>, the sharp singlet at  $\delta \sim 3.45$  ppm is due to the protons of the ethylene oxide units of PEO [-(CH<sub>2</sub>-CH<sub>2</sub>-O)-], and the signal at  $\delta \sim 1.0$ –1.1 ppm corresponds to the methyl groups of PPO [-(CH(CH<sub>3</sub>)-CH<sub>2</sub>-O)-] (Figure S3A). In addition, the characteristic signals of EFV aromatic protons at  $\delta \sim 7.0$ –7.6 ppm are observed. In D<sub>2</sub>O, a deficient solvent for both the core and the drug, the signal attributed to the protons of the hydrophobic PPO is still visible, though the relative intensity to PEO decreased significantly. More important, the signals assigned to EFV disappeared almost completely, indicating that the drug is hosted by the micellar core almost exclusively (Figure S3B).

T904-containing mixed micelles displayed a statistically significant increase of the encapsulation capacity with respect to pF127 (one-way ANOVA  $P < 0.05$ ; Dunnett Multiple Comparison Test  $P < 0.01$ ). For example, F127:T904 (50:50) and (25:75) increased the S<sub>a</sub> 7820- and 8432-times, respectively, and pF127 showed a more modest 4873-fold (Table 5). Moreover, the value of 25:75 represented an additional

Table 5

Apparent solubility ( $S_a$ ) and solubility factors ( $f_s$ ) of EFV within mixed micellar systems (pH 5), at 25°C

Copolymers	EFV in micellar systems (10%)		
	$S_a$ (mg/mL)	$f_s$ ( $\pm$ S.D.)	$P$ value*
pF127	19.49 (3.30)	4873.3 (826.0)	-
F127 7.5% + T304 2.5% <sup>†</sup>	14.69 (2.42)	3672.0 (604.7)	-
F127:T304 (75:25) <sup>‡</sup>	16.40 (0.82)	4098.9 (205.8)	N.S.
F127 5% + T304 5% <sup>†</sup>	9.88 (1.53)	2470.7 (383.4)	-
F127:T304 (50:50) <sup>‡</sup>	10.87 (0.46)	2718.3 (114.7)	N.S.
F127 2.5% + T304 7.5% <sup>†</sup>	5.08 (0.65)	1269.3 (162.2)	-
F127:T304 (25:75) <sup>‡,§</sup>	7.27 (0.92)	1817.7 (230.0)	0.0279
pT304	0.41 (0.03)	102.0 (7.1)	-
F127 7.5% + T904 2.5% <sup>†</sup>	22.55 (2.33)	5637.6 (582.1)	-
F127:T904 (75:25) <sup>‡</sup>	26.16 (4.28)	6539.0 (1069.3)	N.S.
F127 5% + T904 5% <sup>†</sup>	25.61 (1.07)	6401.9 (268.4)	-
F127:T904 (50:50) <sup>‡,§</sup>	31.28 (2.35)	7819.7 (587.6)	0.0191
F127 2.5% + T904 7.5% <sup>†</sup>	28.66 (2.33)	7166.2 (418.4)	-
F127:T904 (25:75) <sup>‡,§</sup>	33.73 (1.49)	8432.4 (371.9)	0.0173
pT904	31.72 (2.97)	7930.5 (741.7)	-

All the mixed micelles showed statistically significant difference ( $P < 0.05$ ) of EFV solubility in comparison with the solubility in pF127, with the exception of F127:T304 (75:25).  $P$  values correspond to the comparison of the mixed micelle with the corresponding theoretical mixture calculated as the sum of the EFV amounts solubilized in each pure micellar system.

N.S., differences are not statistically significant;  $S_a$ , EFV apparent solubility;  $f_s$ , EFV solubility factor.

\* Unpaired  $t$ -test ( $P < 0.05$ ).

<sup>†</sup> Solubility calculated as the sum of EFV amounts solubilized in the pure micellar system of the corresponding copolymer; i.e., F127 7.5%+T304 2.5% represents the sum of the amounts of EFV solubilized in 7.5% F127 system and 2.5% T304 pure systems.

<sup>‡</sup> Mixed micelles

<sup>§</sup> Differences are statistically significant with respect to the corresponding theoretical mixture.

improvement of the performance shown by pT904. In contrast, the addition of T304 to F127 (in any ratio) had a detrimental effect,  $S_a$  being always substantially lower than that of pF127. The greater the T304 content, the lower the encapsulation extent observed; e.g.,  $f_s$  values for 50:50 and 25:75 systems were 2718 and 1818, respectively (Table 5). All the binary systems displayed a greater solubilization extent than the corresponding theoretical mixture calculated as the sum of the EFV amounts solubilized in the pure micellar system of the corresponding copolymer. For example, F127:T304 (25:75) showed  $S_a$  of 7.27 mg/mL, and the sum of  $S_a$  corresponding to pF127 2.5% and pT304 7.5% was 5.08 mg/mL (Figure 3, A); the difference was statistically significant (unpaired  $t$ -test,  $P = 0.0279$ ). Similarly, F127:T904 (50:50) and (25:75) showed  $S_a$  values of 31.28 and 33.73 mg/mL as opposed to the corresponding sums of 25.61 and 28.66 mg/mL (Figure 3, B); again, differences were statistically significant (unpaired  $t$  test,  $P$  values were 0.0191 and 0.0173, respectively).

#### Effect of EFV encapsulation on the size of the aggregates

The size and size distribution of 10% pure and mixed EFV-loaded micelles were studied by DLS at 25° and 37°C (Figure 4).

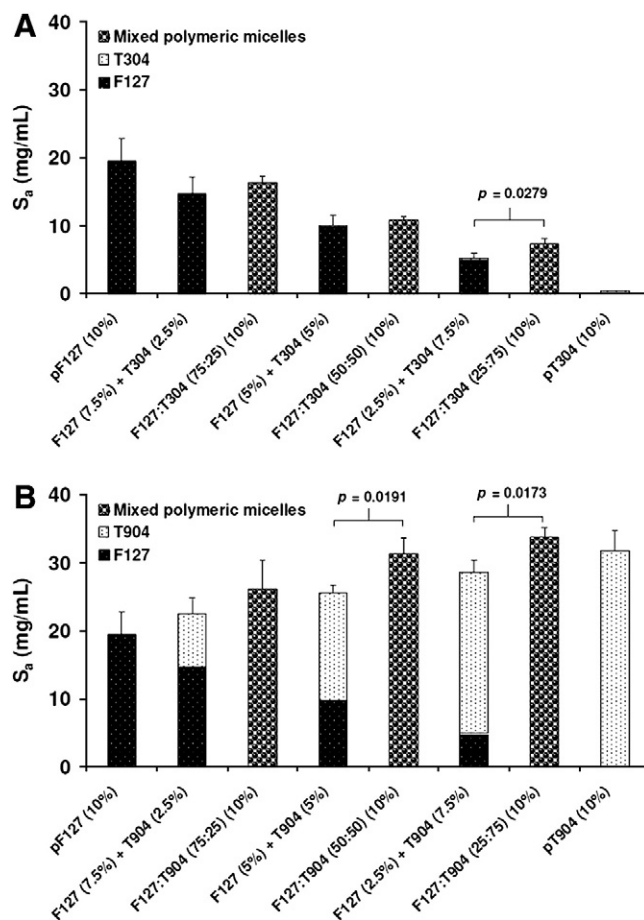


Figure 3. Apparent solubility ( $S_a$ ) of EFV in the different micellar systems (A) F127:T304 and (B) F127:T904. Error bars represent S.D. ( $n = 3$ ).

\* Statistically significant difference between systems (unpaired  $t$  test,  $P < 0.05$ ).

In general, the encapsulation of EFV led to the disappearance of the small-size fraction (unimers and incomplete aggregates) present in all the drug-free micelles at 25°C. For example, F127:T304 (75:25), (50:50) and (25:75) showed  $D_h$  of 24, 33 and 42 nm, respectively (Figure 4, panels B-D), sizes being similar to those of the drug-free systems (Table 3). Conversely, pF127 and pT304 presented a bimodal distribution with a remanent population of small structures (3–4 nm) and a main size fraction comprised of aggregates with  $D_h$  of 24 and 400 nm, respectively (Figure 4, panels A,E). A similar behavior was observed for F127:T904 systems (Figure 4, panels F-I). These  $D_h$  values were slightly smaller than those of EFV-containing pT904 micelles. In addition, specimens remained transparent (Figure 4, photo insets, panels A-I).

At 37°C, a similar trend was apparent and in general drug-loaded micelles displayed sizes similar to those shown by drug-free ones (Figure 4). However, pT304 still showed two size populations. In T904-containing mixtures, two different behaviors were observed. Although 75:25 and 50:50 conserved the properties of drug-free systems and sizes remained below 20 nm, F127:T904 (25:75) and pT904 systems formed remarkably larger structures of 255 nm and 1.1  $\mu$ m upon heating, these samples becoming opalescent (Figure 4, panels H, I).<sup>29</sup>



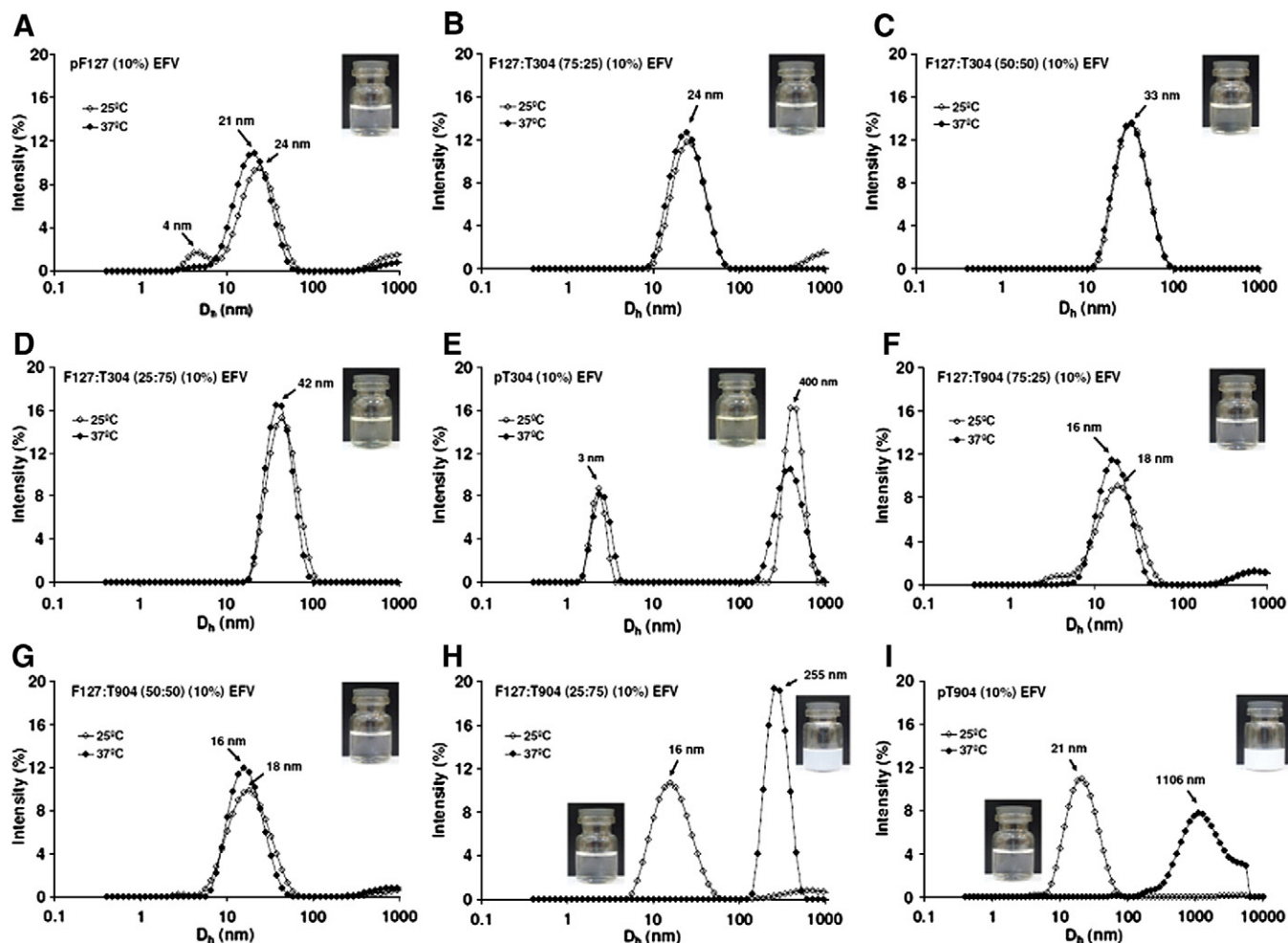


Figure 4.  $D_h$  and size distribution of EFV-loaded micellar systems, at 25 and 37°C. Photo insets show the appearance of the drug-loaded systems. In general, the encapsulation of EFV led to the disappearance of the small-size fraction (unimers and incomplete aggregates) present in all the drug-free micelles at 25°C.

#### Physicochemical stability of the drug-containing micelles

Specimens were stored at 4° and 25°C and the EFV content and the micellar size and size distribution monitored over 28 days. At 4°C, pT904 was very unstable, %EFV being approximately 40% at day 7 (Figure 5, A). F127:T304 (25:75) and F127:T904 (50:50) were slightly more stable and showed a concentration drop between days 7 and 14. F127:T904 (25:75) showed a decrease between days 21 and day 28. These findings indicate the stabilization performance of F127. At 25°C, all the EFV-loaded micelles showed higher physical stability (EFV% > 90%) (Figure 5, B). These results were consistent with an increased micellization tendency upon heating. DLS confirmed that sizes remained unchanged at 25°C (Figure 6, A–H); note that size distributions were superimposable.

#### Discussion

Developing highly concentrated aqueous formulations of EFV and more novel poorly water-soluble anti-HIV drugs represents a primary goal to improve the pharmacotherapy of the pediatric population.<sup>11</sup>

The hypothesis of this study was that the co-micellization of the highly hydrophilic F127 with more hydrophobic amphiphiles would enhance the EFV encapsulation capacity, while maintaining the high physical stability of pF127 micelles; EFV-loaded pure T904 micelles are less physically stable. In addition, we expected to maintain the size of the drug-loaded nanocarriers to be sufficiently small to ensure the appropriate absorption in the intestine after oral administration (Figure 7).

To generate mixed poloxamer/poloxamine polymeric micelles by means of a co-micellization process, both amphiphiles need to display hydrophobic segments of similar molecular weight, though a different hydrophilic/hydrophobic balance.<sup>32,33</sup> In this study, we explored and thoroughly characterized for the first time the generation of mixed poloxamer/poloxamine micelles. The impact of introducing a poloxamine resides in the greater chemical versatility of these branched counterparts. In a recent work, we proposed that poloxamine molecules would behave as two PEO-PPO-PEO triblocks linked in the center by the ethylenediamine group<sup>39</sup>; poloxamines display a fragmented molecular architecture where the PPO content is the sum of 4 arms (Table 1). In this context, F127 and T904, two copolymers containing approximately 4 kDa PPO/molecule do not comply

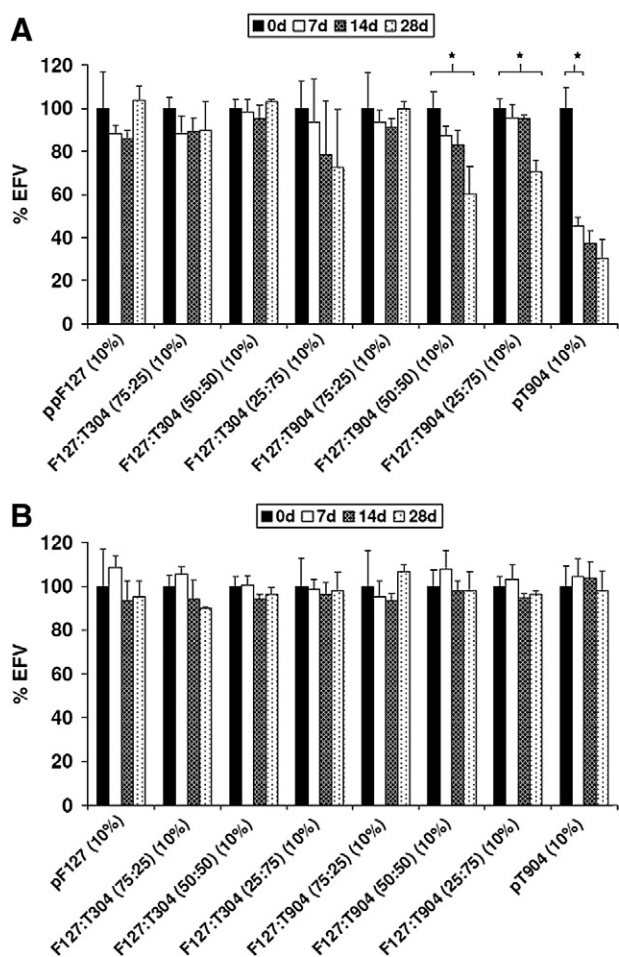


Figure 5. Remaining percentage of efavirenz (%EFV) in solution in different copolymer micellar systems stored over 28 days, at (A) 4°C and (B) 25°C. \*Statistically significant decrease ( $P < 0.05$ ) of the EFV concentration when compared to the initial EFV concentration of the system.

with the general rule stated for the generation of mixed micelles. The same is true for T304.

The self-assembly was characterized in terms of the CMC by DLS as it is a more sensitive and reliable methodology for poloxamers than surface tension.<sup>40</sup> The CMC of F127 (0.24 mM) was very similar to the value reported by Sharma et al using the same technique, 0.20 mM.<sup>41</sup> Theoretical and experimental CMC data were in good agreement at both temperatures (Table 2). However, at 25°C, all the mixtures (with the exception of F127:T904 75:25) displayed a clear positive deviation from ideality; the higher the poloxamine content was, the greater the deviation. At 37°C, a similar trend was apparent. On the other hand, for 75:25 and 50:50 F127:T304 micelles the deviation was negative, the phenomenon being more pronounced for lower poloxamine contents. Mixed systems formed by F127:P85 and F127:P123 also exhibited this positive deviation, and F88:P123 presented a negative one.<sup>35</sup> Positive and negative deviations from ideality suggest unfavorable and favorable mixing processes, respectively. When unfavorable interactions are strong enough, they curtail micellization and lead to greater CMC values. Increasing poloxamine amounts resulted in a steady increase of the CMC,

suggesting that the incorporation of poloxamine into F127 micelles has a moderate deleterious effect on the poloxamer self-aggregation. On the other hand, almost all the binary systems displayed CMC values that were lower than those of the pure poloxamine, stressing the beneficial effect of F127 towards micellization. Because the total copolymer concentration employed in the encapsulation of EFV was far above the CMC values measured, the presence of micelles is ensured.

The CP of a system is intimately associated with the intermicellar interactions in the binary system and it is expected to differ substantially from that of the pure micelles.<sup>35</sup> In addition, a single CP value constitutes strong evidence of the formation of mixed micelles.<sup>42</sup> The high CP displayed by pF127 relies on the high PEO content (and high hydrophilicity) of this copolymer. Moreover, all the binary samples included in this study showed this behavior, and CP values gradually decreased with growing poloxamine concentrations. These findings were in good agreement with a co-micellization process. As expected, the higher the poloxamine concentration in the mixed micelles, the more hydrophobic the system and the lower the CP observed.

DLS analysis of drug-free micelles at 25°C indicated that pF127 micellized only partially (77%).<sup>25</sup> Conversely, pT904 displayed a major population probably belonging to smaller micelles (Figure S1); T904 displays a smaller molecular weight than F127 and a fragmented architecture. In contrast, T304 did not aggregate.<sup>27</sup> Then, the addition of poloxamines led to a mild to sharp increase of the micellar population to percentages between 80.5% and 94.5%, T304 displaying a stronger effect than T904 displayed. Moreover, F127:T904 (75:25) showed a size comparable to that of pF127 and the disappearance of large T904 aggregates (39 nm). These results strongly suggest the incorporation of T904 molecules into F127 micelles. The presence of a remanent fraction of small structures suggested that, even in the presence of a poloxamine, the self-assembly of F127 at 25°C is not complete. At 37°C, specimens showed monomodal size distributions, sizes being notably smaller than those found at 25°C due to the dehydration of both PPO and PEO blocks upon heating. These data constitute additional evidence of the poloxamer/poloxamine interaction and co-micellization, regardless of the fact that the structural properties of the hydrophobic blocks do not comply with those previously stated.<sup>34,35</sup>

To elucidate the dynamic properties of the nanocarrier and to reveal changes in the hydrophobicity that might stem from the incorporation of the poloxamine, pure and mixed micelles were labelled with a free-radical label and investigated by ESR. The mobility within the micelle governs the drug-release rate, and the hydrophobicity of the microenvironment alters the encapsulation capacity. 5DSA evidences the mobility and rotational motion near the hydrophilic region (micellar corona) and at the interface, and 16DSA describes the mobility deeper inside the aggregate, namely at the corona/core interface and the core.<sup>43</sup> The symmetric three-peak pattern usually displayed by the free radical in aqueous medium undergoes broadening due to its incorporation into the micelles and the phenomenon can be quantified by calculating the parameter  $2T_{\perp}$ . In general,  $2T_{\perp}$  values for both labels were smaller than in buffer (Table 4), reflecting the more restricted mobility of the stearic acid chain within the micelle.  $2T_{\perp}$  values of 5DSA and 16DSA for all the

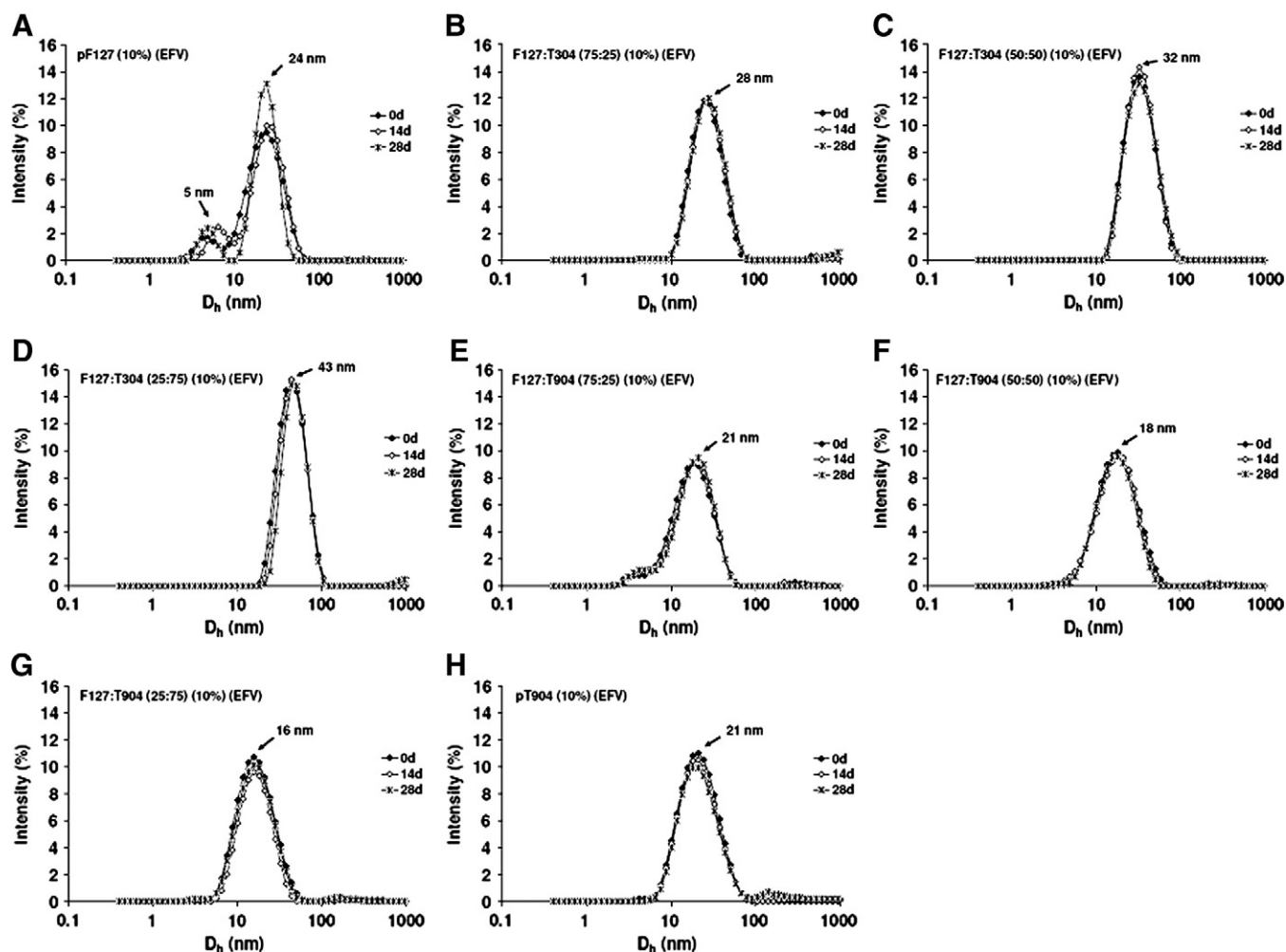


Figure 6.  $D_h$  and size distribution of EFV-loaded micellar systems over 28 days, at 25°C. Sizes remained unchanged; note that size distributions were superimposable.

F127:T304 and F127:T904 binary systems were similar to that of pF127, regardless of the ratio. Moreover,  $2T_{\perp}$  for 5DSA is consistently smaller than 16DSA and suggests that the fluidity within the micelles is lower at the water/corona interface (where the free radical group of 5DSA is located) than in the micellar core. Furthermore,  $a_N$  values were reported as a measure of the micropolarity of the environment surrounding the free radical group. In general, the lower the value is, the more hydrophobic the environment.  $a_N$  values of 5DSA in pF127 and mixed micelles are smaller than in buffer or pure poloxamines. A similar behavior was observed with 16DSA. Because the nitroxide group of 16DSA and 5DSA is in the proximity or within the core and at the water/corona interface, respectively,  $a_N$  values of 16DSA are expected to be lower than those of 5DSA. However, the opposite was apparent. These findings evidenced that this parameter is not fully reliable in the case of our systems. Finally, all  $2T_{\perp}$  and  $a_N$  values for all the mixtures are clearly similar to pF127 (Table 4).

Aiming to gain complementary information regarding the polarity of the micelles and correlate this with the encapsulation capacity of the different systems, an additional assay employing

$K_3Fe(CN)_3$  was conducted. The broadening agent is soluble solely in the aqueous medium and quenches the signal corresponding to more accessible label molecules, namely those that are not incorporated into the micelle or those that are located at the water/micellar corona interface. In contrast, the signal of free radicals staying deep inside the micelle is totally conserved; the quencher cannot interact with them. Results with 16DSA supported that the label is totally incorporated into pF127 and pT904 micelles and all the poloxamer/poloxamine mixtures (Table 4); the nitroxide group is in the inner micellar domain and the broadening agent cannot quench its signal (0% broadening). pT304 does not micellize, resulting in 100% broadening because the label remains exclusively in the aqueous medium. In the case of 5DSA, pT904 totally prevented the quenching phenomenon, and it was quenched approximately 30% in pF127. In other words, the label is more available to  $K_3Fe(CN)_3$  in pF127 than in pT904. Because the incorporation of the label into the micelles is independent of the position of the nitroxide moiety, the complete incorporation of 5DSA to both pF127 and pT904 micelles is assumed. Thus, these data indicate that pF127 micelles are less hydrophobic than those made of



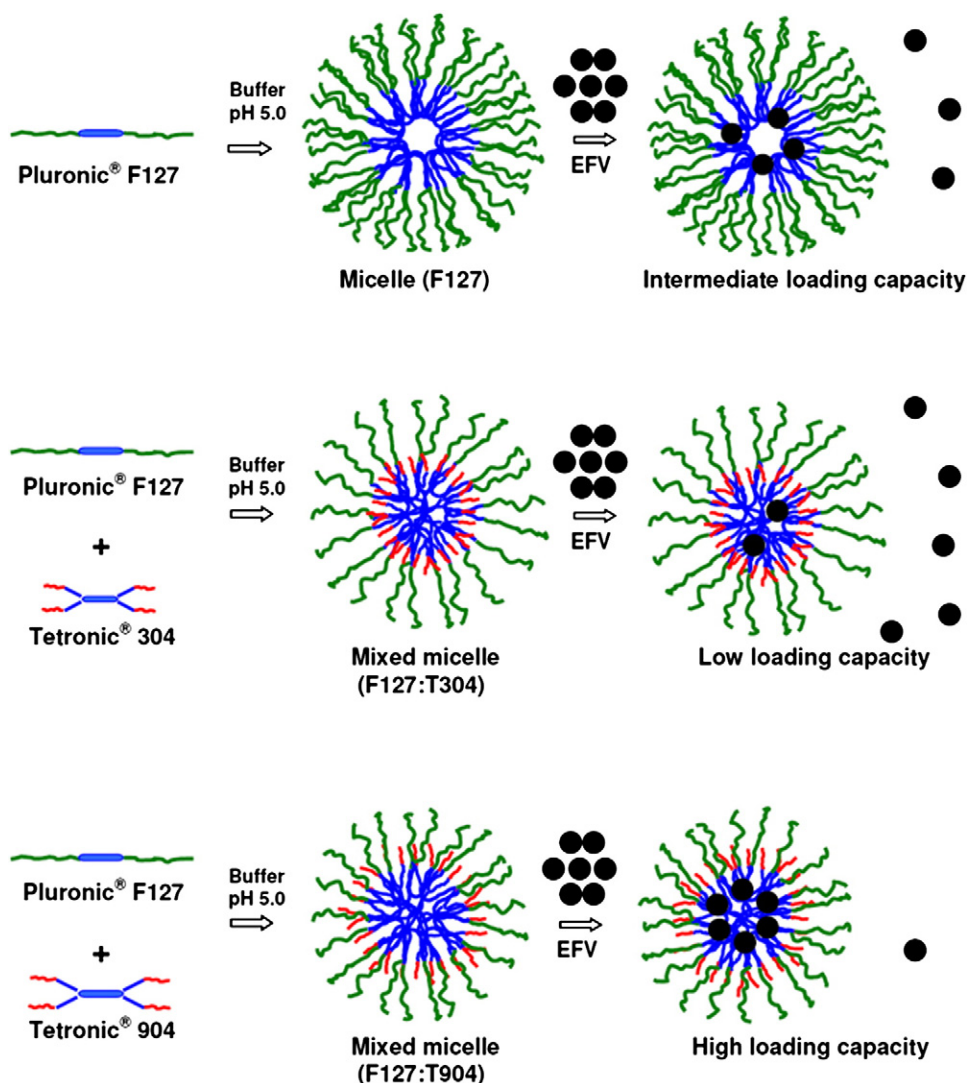


Figure 7. Schematic representation of EFV-loaded pF127 and mixed polymeric micelles (F127:T304 and F127:T904). F127:T904 displayed greater encapsulation efficiency than both pure F127 and T904 counterpart. Conversely, findings suggested that the core of mixed F127:T304 micelles is mainly occupied by T304 molecules that hamper the incorporation of EFV and lead to encapsulation extents lower than pF127 micelles. The generation of the mixed micelles is supported by DLS, CMC, CP and ESR data.

pT904, protecting them less effectively. Increasingly greater T304 amounts in F127:T304 mixed micelles made micelles more hydrophobic. These data suggested that the poloxamine is incorporated into F127 micelles, that in turn become more hydrophobic and “protect” better the label from the quencher. A similar behavior was found in F127:T904 systems, though the quenching percentage showed a more pronounced decrease even with 25% poloxamine. These results would indicate that the formation of F127:T904 is more favored and that micelles rapidly become more hydrophobic, regardless of the poloxamine concentration. Overall ESR data strongly support that the hypothesis that F127 micelles would play the role of “micellar template,” determining the structure of the binary system in terms of size and fluidity. Then, the incorporation of T304 and T904 made the systems more hydrophobic (Figure 7).

In our previous studies, the best encapsulation was attained with 10% pF127 and pT904,  $S_a$  values being approximately 20

and 30 mg/mL, respectively. This concentration fits very well the administration of 200–600 mg in a reasonable volume. Because smaller volumes could improve patient compliance and adherence, an interest exists to augment the drug concentration in solution. Thus, a T904-based formulation would appear to be the most appropriate. However, EFV-loaded T904 systems were physically unstable over time.<sup>30</sup> All the mixed F127:T904 micelles displayed  $S_a$  and  $f_s$  values significantly greater than pF127 (Table 5). These findings are supported by the greater hydrophobicity of F127:T904 micelles, as shown in ESR analysis. Contrary to this, the addition of T304 resulted in a clear deleterious effect,  $S_a$  values being significantly smaller than in pF127. DLS, CP and ESR data revealed that despite the very dissimilar structures the co-micellization of F127/T304 certainly takes place; ESR experiments indicated the greater hydrophobicity of F127:T304 systems with respect to pF127. Thus, the more limited EFV solubilization capacity in F127:T304 binary



systems would stem from the intrinsically inefficient encapsulation capacity of T304. However, other detrimental interactions between EFV and this atypical poloxamine should not be discarded, as previously depicted for pyrene and simvastatin.<sup>27</sup> On the other hand, experimental solubility values were consistently greater than the theoretical ones (Table 5). It seems reasonable to consider that the longer PPO blocks presented by T904 (in comparison with those of T304) contribute to generate larger micellar cores that lead to greater solubilization performances. In any event, these findings confirm the synergistic encapsulation behavior of some of the mixed micelles.

Drug incorporation into the micelles usually leads to micellar enlargement by means of micellar expansion<sup>44,45</sup> or micellar fusion.<sup>46</sup> In this study, the bimodal size pattern shown by drug-free micelles was replaced by a monomodal one of EFV-loaded systems, indicating a more complete micellization due to the presence of EFV.<sup>29</sup>

Temperature fluctuations under controlled or uncontrolled storing conditions could lead to the micellar disassembly and the irreversible precipitation of EFV. Binary systems were more stable than pT904 micelles (Figure 5), the stability being slightly greater for lower poloxamine contents. These findings confirm that F127:T904 mixed micelles combine the advantageous features of both components, that is 1) the greater encapsulation capacity of T904 and 2) the higher physical stability of F127, and support the current approach to produce more concentrated and stable EFV aqueous solution.

Finding the cure for the HIV/AIDS infection appears as a long-term challenge. Meanwhile, reducing the gap between state-of-the-art and “ideal” pediatric formulations is probably one of the most tangible goals to assure a more compliant pharmacotherapy. Our research addresses the matter on two main fronts, namely the technological and the preclinical ones. Both will constitute the most valuable evidence toward the most crucial of the stages that we are planning these days: the clinical one. In this context, the present study stresses the versatility of the scalable and cost-effective PEO-PPO polymeric micelles to fine-tune not only the encapsulation performance but also the size of the drug-loaded aggregates. This issue, which might appear to be irrelevant, can govern the absorption in the gastrointestinal tract and the oral bioavailability.<sup>47,48</sup> Finally, the T904 inhibitory activity on BCRP pumps, an efflux transporter of EFV in the intestine, has been recently revealed in an ex vivo model.<sup>49</sup> In this framework, additional advantageous features can be envisioned for these mixed micelles.

## Appendix A. Supplementary data

Supplementary materials related to this article can be found online at [doi:10.1016/j.nano.2011.01.017](https://doi.org/10.1016/j.nano.2011.01.017).

## References

1. AIDS epidemic update, 2007. World Health Organization. Available from: <http://www.who.int/hiv/epiupdates/en/index.html>. Accessed July 2010.
2. Matic S, Lazarus JV, Donoghoe MC. HIV/AIDS in Europe: moving from death sentence to chronic disease management. World Health Organization Regional Office for Europe. World Health Organization Publications; 2006.
3. Panel of clinical practices for treatment of HIV infection. Pan Am J Public Health 2001;10:426-35.
4. Andrews L, Friedland G. Progress in th HIV therapeutics and the challenges of adherence to antiretroviral therapy. Inf Dis Clin N Amer 2000;14:1-26.
5. Medecins sans Frontieres, Press release, Available from: <http://www.msf.org/>. Accessed July 2010.
6. The U.S. president's emergency plan for AIDS relief (PEPFAR). Pediatric treatment and care. Available from: <http://www.pepfar.gov/pepfar/press/86524.htm>. Accessed June 2010.
7. AIDS orphans, AVERT Organization, 2010. Available from: [www.avert.org/aidsorphans.htm](http://www.avert.org/aidsorphans.htm). Accessed May 2010.
8. Giaquinto C, Morelli E, Fregonese F, Rampon O, Penazzato M, de Rossi A, et al. Current and future antiretroviral treatment options in paediatric HIV infection 1. Clin Drug Invest 2008;28:375-97.
9. Brown E. Antiretroviral therapy in children, HIV/AIDS primary care guide. Chapter 30. AIDS Educ Train Centers Natl Resource Center 2007:419.
10. World Health Organization. Make medicines child size. Available from: <http://www.who.int/childmedicines/en>. Accessed June 2010.
11. Sosnik A. Nanotechnology contributions to the pharmacotherapy of pediatric HIV: a dual scientific and ethical challenge and a still pending agenda. Nanomedicine 2010;5:833-7.
12. Barrueco N, Castillo I, Ais A, Martinez C, Sanjurjo M. Program of pharmaceutical attention to pediatric patients in antiretroviral therapy. Farm Hosp 2005;29:367-74.
13. Wintergerst U, Hoffmann F, Jansson A, Notheis G, Huß K, Kurowski M, et al. Antiviral efficacy, tolerability and pharmacokinetics of efavirenz in an unselected cohort of HIV-infected children. Antimicrob Chemother 2008;61:1336-9.
14. Sosnik A, Chiappetta DA, Carcaboso A. Drug delivery systems in HIV pharmacotherapy: what has been done and the challenges standing ahead. J Control Release 2008;138:2-15.
15. Friedland G, Khoo S, Jack C, Lalloo U. Administration of efavirenz (600 mg/day) with rifampicin results in highly variable levels but excellent clinical outcomes in patients treated for tuberculosis and HIV. J Antimicrob Chemother 2006;58:1299-302.
16. Fabbiani M, Di Giambenedetto S, Bracciale L, Bacarelli A, Ragazzoni E, Cauda R, et al. Pharmacokinetic variability of antiretroviral drugs and correlation with virological outcome: 2 years of experience in routine clinical practice. J Antimicrob Chemother 2009;64:109-17.
17. van Luin M, Gras L, Richter C, van der Ende ME, Prins JM, de Wolf F, et al. Efavirenz dose reduction is safe in patients with high plasma concentrations and may prevent efavirenz discontinuations. J Acquir Immune Defic Syndr 2009;52:240-5.
18. Wintergerst U, Hoffmann F, Jansson A, Notheis G, Huss K, Kurowski M, et al. Antiviral efficacy, tolerability and pharmacokinetics of efavirenz in an unselected cohort of HIV-infected children. J Antimicrob Chemother 2008;61:1336-9.
19. Bahal SM, Romansky JM, Alvarez FJ. Medium chain triglycerides as vehicle for palatable oral liquids. Pharm Dev Technol 2003; 8:111-5.
20. Sellers RS, Antman M, Phillips J, Khan KN, Furst SM. Effects of Miglyol 812 on rats after 4 weeks of gavage as compared with methylcellulose/Tween 80. Drug Chem Toxicol 2005;28:423-32.
21. Administración Nacional de Medicamentos, Alimentos y Tecnología Médica (ANMAT), Ministry of Health, Argentina. Available from: [www.anmat.gov.ar](http://www.anmat.gov.ar). Accessed May 2010.
22. Chiappetta DA, Carcaboso AM, Rubio MC, Bramuglia G, Sosnik A. Indinavir-loaded pH-sensitive microparticles for taste masking: toward extemporaneous pediatric anti-HIV/AIDS liquid formulations with improved patient compliance. AAPS Pharm Sci Tech 2009;10:1-6.

23. Sosnik A, Amiji M. Nanotechnology solutions for infectious diseases in developing nations. *Adv Drug Del Rev* 2010;62:375-7.
24. Sosnik A, Carcaboso AM, Chiappetta DA. Polymeric nanocarriers: new endeavors for the optimization of the technological aspects of drugs. *Recent Pat Biomed Eng* 2008;1:43-59.
25. Chiappetta DA, Sosnik A. Poly(ethylene oxide)–poly(propylene oxide) block copolymer micelles as drug delivery agents: improved hydro-solubility, stability and bioavailability of drugs. *Eur J Pharm Biopharm* 2007;66:303-17.
26. Chiappetta DA, Degrossi J, Teves S, D’Aquino M, Bregni C, Sosnik A. Triclosan-loaded poloxamine micelles for enhanced topical antibacterial activity against biofilm. *Eur J Pharm Biopharm* 2008;69:535-45.
27. Gonzalez-Lopez J, Alvarez-Lorenzo C, Taboada P, Sosnik A, Sandez-Macho I, Concheiro A. Self-associative behavior and drug-solubilizing ability of poloxamine (tetronic) block copolymers. *Langmuir* 2008;24:10688-97.
28. Chiappetta DA, Hocht C, Taira C, Sosnik A. Efavirenz-loaded polymeric micelles for pediatric anti-HIV pharmacotherapy with significantly higher oral bioavailability. *Nanomedicine* 2010;5:11-23.
29. Chiappetta DA, Alvarez-Lorenzo C, Rey-Rico A, Taboada P, Concheiro A, Sosnik A. N-alkylation of poloxamines modulates micellar encapsulation and release of the antiretroviral efavirenz. *Eur J Pharm Biopharm* 2010;76:24-37.
30. Chiappetta DA, Hocht C, Sosnik A. A highly concentrated and taste-improved aqueous formulation of efavirenz for a more appropriate paediatric management of the anti-HIV therapy. *Curr HIV Res* 2010;8:23-31.
31. Oh KT, Bronich TK, Kabanov AV. Micellar formulations for drug delivery based on mixtures of hydrophobic and hydrophilic Pluronic® block copolymers. *J Control Release* 2004;94:411-22.
32. Wei Z, Hao J, Yuan S, Li Y, Juan W, Sha X, et al. Paclitaxel-loaded Pluronic P123/F127 mixed polymeric micelles: formulation, optimization and in vitro characterization. *Int J Pharm* 2009;376:176-85.
33. Li L, Tan YB. Preparation and properties of mixed micelles made of Pluronic polymer and PEG-PE. *J Colloid Interface Sci* 2008;317: 326-31.
34. Nandni D, Vohra KK, Mahajan RK. Study of micellar and phase separation behavior of mixed systems of triblock polymers. *J Colloid Interface Sci* 2009;338:420-7.
35. Clint JH. Micellization of mixed nonionic surface active agents. *J Chem Soc Faraday Trans* 1975;1:1327-34.
36. Pandit N, Trygstad T, Croy S, Bohorquez M, Koch C. Effect of salts on the micellization, clouding, and solubilization behavior of pluronic F127 solutions. *J Colloid Interface Sci* 2000;222:213-20.
37. Lurie DJ, Mäder K. Monitoring drug delivery processes by EPR and related techniques—principles and applications. *Adv Drug Deliv Rev* 2005;57:1171-90.
38. Kempe S, Metz H, Mäder K. Application of Electron Paramagnetic Resonance (EPR) spectroscopy and imaging in drug delivery research – Chances and challenges. *Eur J Pharm Biopharm* 2010;74:55-66.
39. Alvarez-Lorenzo C, Rey-Rico A, Brea J, Loza MI, Concheiro A, Sosnik A. Inhibition of P-glycoprotein pumps by PEO-PPO amphiphiles: branched versus linear derivatives. *Nanomedicine* 2010;5:1371-83.
40. Bakshi MS, Bhandari P, Sachar S, Mahajan RK. Mixed micelles of binary triblock polymer mixtures in pure water at 30°C. *Colloid Polym Sci* 2006;284:1363-70.
41. Sharma PK, Reilly MJ, Jones DN, Robinson, Bhatia SR. The effect of pharmaceuticals on the nanoscale structure of PEO–PPO–PEO micelles. *Colloids Surf B: Biointerfaces* 2008;61:53-60.
42. Cardoso da Silva R, Loh W. Effect of additives on the cloud points of aqueous solutions of ethylene oxide–propylene oxide–ethylene oxide block copolymers. *J Colloid Interface Sci* 1998;202:385-90.
43. van den Bergh BAI, Wertz PW, Junginger HE, Bouwstra JA. Elasticity of vesicles assessed by electron spin resonance, electron microscopy and extrusion measurements. *Int J Pharm* 2001;217:13-24.
44. Riess G. Micellization of block copolymers. *Prog Polym Sci* 2003;28:1107-70.
45. Allen C, Maysinger D, Eisenberg A. Nano-engineering block copolymer aggregates for drug delivery. *Colloids Surf B* 1999;16:3-27.
46. Xu RL, Winnik MA, Hallett FR, Riess G, Croucher MD. Light-scattering study of the association behavior of styrene-ethylene oxide block copolymers in aqueous solution. *Macromolecules* 1991;24:87-93.
47. Mathot F, des Rieux A, Arien A, Schneider YJ, Brewster M, Preat V. Transport mechanisms of mmePEG(750)P(CL-co-TMC) polymeric micelles across the intestinal barrier. *J Control Release* 2007;124:134-43.
48. Chiappetta DA, Hocht C, Taira C, Sosnik A. Oral pharmacokinetics of efavirenz-loaded polymeric micelles. *Biomaterials* 2011;32:2379-87.
49. Peroni RN, Hocht C, Chiappetta DA, Di Gennaro SS, Rubio MC, Sosnik A, et al. The anti-HIV drug efavirenz is substrate and modulates the expression of the efflux transporter BCRP (ABCG2) in rats. *First World Conference on Nanomedicine and Drug Delivery (WCN2010)*. India: Kottayam; 2010.